

AperTO - Archivio Istituzionale Open Access dell'Università di Torino

Evolutionary dynamics in club goods binary games

This is a pre print version of the following article:

Original Citation:

Availability:

This version is available <http://hdl.handle.net/2318/1681260> since 2018-11-15T11:48:24Z


Terms of use:

Open Access

Anyone can freely access the full text of works made available as "Open Access". Works made available under a Creative Commons license can be used according to the terms and conditions of said license. Use of all other works requires consent of the right holder (author or publisher) if not exempted from copyright protection by the applicable law.

(Article begins on next page)

AUTHOR QUERY FORM

	Journal: DYNCON Article Number: 3559	Please e-mail your responses and any corrections to: E-mail: correctionsaptara@elsevier.com
---	---	--

Dear Author,

Please check your proof carefully and mark all corrections at the appropriate place in the proof (e.g., by using on-screen annotation in the PDF file) or compile them in a separate list. Note: if you opt to annotate the file with software other than Adobe Reader then please also highlight the appropriate place in the PDF file. To ensure fast publication of your paper please return your corrections within 48 hours.

Your article is registered as belonging to the Special Issue/Collection entitled “Carl Chiarella”. If this is NOT correct and your article is a regular item or belongs to a different Special Issue please contact k.applegate@elsevier.com immediately prior to returning your corrections.

For correction or revision of any artwork, please consult <http://www.elsevier.com/artworkinstructions>

Any queries or remarks that have arisen during the processing of your manuscript are listed below and highlighted by flags in the proof. Click on the ‘[Q](#)’ link to go to the location in the proof.

Location in article	Query / Remark: click on the Q link to go Please insert your reply or correction at the corresponding line in the proof		
Q1	AU: The author names have been tagged as given names and surnames (surnames are highlighted in teal color). Please confirm if they have been identified correctly.		
Q2	AU: Please provide complete information of authors’ affiliation.		
Q3	AU: Please check funding agency and confirm their correctness.		
	<table border="1"><tr><td>Please check this box or indicate your approval if you have no corrections to make to the PDF file</td><td></td></tr></table>	Please check this box or indicate your approval if you have no corrections to make to the PDF file	
Please check this box or indicate your approval if you have no corrections to make to the PDF file			

Thank you for your assistance.



Contents lists available at ScienceDirect

Journal of Economic Dynamics & Control

journal homepage: www.elsevier.com/locate/jedc

Evolutionary dynamics in club goods binary games

Gian Italo Bischi^{a,*}, Ugo Merlone^b, Eros Pruscini^a^a Università di Urbino Carlo Bo, Italy^b Università di Torino, Italy

ARTICLE INFO

Article history:

Received 26 April 2017

Revised 26 November 2017

Accepted 5 February 2018

Available online xxx

Keywords:

Binary games

Social externalities

Club goods

Discrete dynamical systems

Replicator dynamics

Global bifurcations

ABSTRACT

A dynamic adjustment mechanism, based on replicator dynamics in discrete time, is used to study the time evolution of a population of players facing a binary choice game with social influence, characterized by payoff curves that intersect at two interior points, also denoted as thresholds. So, besides the boundary equilibria where all players make the same choice, there are two further steady states where agents playing different strategies coexist and get identical payoffs. Such binary game can be interpreted as a club good game, in which players have to choose either joining or not the club in the presence of cost sharing, so that they can enjoy a good or a service provided that a “participation” threshold is reached. At the same time congestion occurs beyond a second higher threshold. These binary choice models, can be used (and indeed have been used in the literature) to represent several social and economic decisions, such as technology adoption, joining a commercial club, R&D investments, production delocalization, programs for environmental protection. Existence and stability of equilibrium points are studied, as well as the creation of more complex attractors (periodic or chaotic) related with overshooting effects. The study of some local and global dynamic properties of the evolutionary model proposed reveals that the presence of the “participation” threshold causes the creation of complex topological structures of the basins of coexisting attracting sets, so that a strong path dependence is observed. The dynamic effects of memory, both in the form of convex combination of a finite number of previous observation (moving average) and in the form of memory with increasing length and exponentially fading weights are investigated as well.

© 2018 Elsevier B.V. All rights reserved.

1. Introduction

2 Concepts like bounded rationality, social influence, evolution, imitation, underlay the recent developments of behavioral
 3 economics (for a review on behavioral economics the reader may consult Camerer and Loewenstein, 2004 and Thaler, 2016).
 4 However, well before the recent success of this discipline, Schelling (1973) studied situations in which choices between two
 5 alternatives are influenced by social interactions, and named such situations “binary choices with externalities”. Through
 6 lively and memorable examples (see e.g. Dixit, 2006) he qualitatively described stylized situations where social influence
 7 affects choices not by direct strategic interaction rather via externalities (Laffont, 2008). This way, although individuals are
 8 concerned about their own interest (unbounded selfishness, see Thaler and Mullainathan, 2001), others’ action have an im-
 9 pact on their payoffs. The consequences of these interactions are connected to complexity Arthur (2013) and it is interesting
 10 to study the patterns in collective behavior emerging from the interdependence generated by externalities.

* Corresponding author.

E-mail address: gian.bischi@uniurb.it (G.I. Bischi).

Collective behavior has been studied by several disciplines such as sociology (Granovetter and Soong, 1983), politics (Hovi, 1986), social psychology (Allport, 1924), industrial organization (Fazeli and Jadbabaie, 2012), marketing (Mahajan et al., 1990), and communication (van Ginneken, 2003) to name a few. In fact, according to Granovetter (1978), several processes such as residential segregation, voting, crowd behavior, diffusion of innovations and consumption choices can be considered as situations in which people adopt new norms and abandon existing ones.

When assuming that binary decisions can be repeatedly modified over time, such models are particularly meaningful in a dynamic setting, where an evolutive adaptive process is introduced to mimic how agents switch from one choice to another according to the observed payoff differences.

Dynamic binary games expressed in the form of piecewise differentiable discrete dynamical systems, have been studied in Bischi and Merlone (2009, 2010), where different kinds of long run behaviors have been evidenced, such as convergence to an equilibrium situation or endless self-sustained endogenous oscillations, either periodic or chaotic. However, as explained in Bischi and Merlone (2017), order to describe how groups of individuals within a population change their strategy over time based on payoff comparisons, it is more convenient to consider an evolutionary games approach. Therefore, a discrete-time evolutionary model, based on replicator dynamics in the form proposed by Cabrales and Sobel (1992) (see also Hofbauer and Sigmund, 2003) has been proposed in Bischi and Merlone (2017) to describe minority games, i.e. situations where payoff curves intersect at a given “congestion” threshold such that a higher payoff is gained by agents choosing the less selected strategy. In this paper the same evolutionary approach is followed to investigate the case of payoff curves with two intersections: an higher intersection representing a “congestion” threshold similar to the one existing in a minority game and a lower threshold representing a “participation” threshold that marks a level of selection of a strategy below which the same strategy is dominated, i.e. its payoff is lower, like in an economic system characterized by increasing returns, (Arthur, 1994). Such a situation may be referred as a club good game, in which players have to choose either joining or not the club in the presence of cost sharing, so that they can enjoy a good or a service provided that a participation threshold is reached. At the same time congestion occurs beyond a second higher threshold. These models are quite common in the economic and social literature, for example for the description of a population of economic agents that decide, at each time step, if they want to contribute or not to a public project which is launched if and only if a certain level of contributions is reached, as well as other similar situations including taxation, Research and Development (R&D) expenditures, etc. (see e.g. Bolle, 2014; Schelling, 1973; Granovetter, 1978 for several examples of such binary games). In order to model such a general dynamic framework, we consider the case of two different options, denoted by R and L , characterized by payoff functions $R(x)$ and $L(x)$ respectively, which depend on the fraction x of the population of players making a given choice, say R (L being chosen by the complementary fraction $1 - x$) with just two intersection, or thresholds, to represent cases where L is more convenient (or dominant) for low and high values of x and R is preferred for intermediate values of x . To give a general interpretation of this framework, let the option R represent the choice of an individual of getting a given club good or service, i.e. a good or service both excludable and rival¹ (Mankiw and Taylor, 2014, p. 222). In fact, goods can be classified in terms of their exclusive use and how being used by more consumers may decrease their cost, due to sharing cost effects, see Buchanan (1965). Moreover, Buchanan (1965) when closing the gap between the purely public and the purely private goods, considers total cost and total benefit per person using the good and specifically introduces a point in which congestion sets in and the evaluation of the good falls.

Several cases of binary choices with these two threshold levels can be found in the literature. For example, Bolle (2014) considers the decision of limiting environmental pollution. On one hand, if nobody (or very few) will reduce pollution then the isolate decision of an agent to reduce pollution is useless. On the other hand, if most agents stick to the decision of not polluting then environment condition will improve enough even without all the agents joining this decision. In both cases the total cost is larger than the total benefit for the agents deciding to limit environmental pollution. By contrast, when the fraction of agents limiting environmental pollution lies between these two thresholds the benefit coming from lower environmental pollution is larger than the cost of reducing pollution.

Another meaningful example is given when considering the trade-off between R&D expenditures and knowledge spillovers among firms producing similar goods in an industrial district (see e.g. Bischi et al., 2003a; Bischi et al., 2003b; Bischi and Lamantia, 2002). In order to produce and sell a given product, R&D investments may be quite inefficient if nobody else produces the same good, because no know-how exists – for example it may be difficult to recruit workers with proper training. By contrast, it is well known that in the framework of an industrial district, where a few firms produce similar goods R&D expenditures are more effective given the positive cost externalities Marshall (1920). Finally, in an industrial districts where the majority of firms produce the same good and invest in R&D, a single firm may take advantage, for free, of the competitor’s R&D results, due to the difficulties to protect intellectual properties and to avoid spillovers of skilled workers among competing firms. As a final example, when assuming that social interactions are among the internal motives associated with attending events (Benckendorff and Pearce, 2012; Morgan, 2009) we can extend the El Farol bar minority game (Arthur, 1994) by introducing a lower threshold to mimic the fact that the presence of just a few people in the bar makes it unattractive.

¹ We recall that a good is *excludable* when “a person can be prevented from using it when she does not pay for it” (Mankiw and Taylor, 2014, p. 222) and it is called *rival* when “one person use diminishes other people use” (Mankiw and Taylor, 2014, p. 222).

67 These are just a few among several economic and social examples that can be described by payoff functions with two
68 internal intersections, so a study of the dynamic scenarios generated in this case may be useful. As it will become clearer
69 in the following, an important consequence of the presence of the lower “club participation” threshold is the occurrence of
70 a severe path dependence due to the creation of complicated structures of the basins of coexisting attractors. Such global
71 dynamic effects of the dynamical systems we are going to consider are mathematically interesting since they give useful
72 information on some typical nonlinear effects. In this paper we show that such complex behaviors are related to the folding
73 properties of noninvertible dynamical systems that may cause the creation of particular structures of the basins of attraction
74 leading to extreme forms of path dependence.

75 Effects of nonlinearity in economic modelling have been extensively studied in the literature, one of the pioneering books
76 in this field being Chiarella (1990), whereas recent surveys that give the latest trends of nonlinear economic dynamics, in
77 particular with reference to global methods based on a continuous dialogue between analytic, graphical and numerical
78 tools can be found in the volumes of collected papers (Bischi et al., 2010; 2012; Dieci et al., 2014). In the spirit of such
79 stream of literature, this paper tries to join a standard evolutionary model of binary choices with methods for the study of
80 global dynamics, and we show that the presence of the lower “club participation” threshold may give rise to several kinds
81 of long run dynamics, ranging from convergence to a pure strategy with all agents making the same choice to different
82 mixed strategies situations, with stationary or oscillatory (periodic or chaotic) patterns. In this paper we show that such
83 coexistence may be associated with the occurrence of global bifurcations leading to complex topological structures of the
84 basins of attraction, hence a strong path dependence, that can be described in terms of critical sets, a tool for the analysis
85 of global dynamics of noninvertible maps (Agliari et al., 2002; Mira et al., 1996).

86 In this paper we also address another intriguing topic, which is often studied in this context, related to the effects of
87 memory or the presence of time lags in the decision process, i.e. the players’ decisions are not only based on the current
88 payoffs observed, but they take account of payoffs observed in the past as well. Indeed, the effect of memory reveals to
89 be not univocal, as several ambiguous conclusions can be found in the literature (a comparison of the titles of references
90 Cavagna, 1999 and Challet and Marsili, 2000 is quite emblematic). In the context of minority games the problem of memory
91 has been recently analyzed in Dindo (2005) and Bischi and Merlone (2017), whereas more references exist in oligopoly mod-
92 elling, see e.g. Chiarella (1991), Chiarella and Szidarovszky (2003), Chiarella and Szidarovszky (2004). Following Bischi and
93 Merlone (2017), besides the classical replicator dynamics with no memory, we also consider the case in which decisions are
94 taken by using a convex combination of the current observation and some previous ones, i.e., a sort of moving average.

95 To sum up, the aim of this paper is threefold: we introduce a club participation (or sharing cost) threshold in minority
96 games linking these kinds of interactions to the contributions on club goods; we analyze the dynamics of a binary choice
97 model with two threshold values, both without and with memory, that represents several economic and social applications,
98 compared with the analogous models analyzed in the case of a single threshold (namely, minority games, see Bischi and
99 Merlone, 2017); and, finally, we provide an exemplary application of methods to study the global bifurcations leading to the
100 creation of complex topological structures of the basins of attraction.

101 The paper is organized as follows. Section 2 presents the basic setup of the model of repeated binary game with
102 evolutionary dynamics based on exponential replicator, and results on local and global dynamic properties of such one-
103 dimensional dynamic model are given. Section 3 proposes the generalization of the model by considering a finite memory
104 of length 1, and analyzes the corresponding two-dimensional map to investigate the effects of memory on local stability
105 of equilibrium points as well as the global analysis of the basins and the global (or contact) bifurcations that change their
106 topological structure. Then, in Section 4, infinite and exponentially discounted memory is introduced and the corresponding
107 dynamical system is again reduced to an equivalent two-dimensional map. Finally, the last section is devoted to some con-
108 cluding remarks about the economic meaning of the results through a comparison with the economic and social literature.

109 2. The model of binary choice with replicator dynamics

110 2.1. Dynamic model setup

111 Let us consider a population of players, each facing a binary choice between strategies R and L , and let $x(t) \in [0, 1]$ be the
112 fraction of agents playing R at time period t (consequently the complementary fraction $1 - x(t)$ plays L at the same time
113 period). The individual payoff of an agent employing a given strategy at time t is assumed to depend only on the number
114 of agents making the same choice, say $R(t) = R(x(t))$ and $L(t) = L(x(t))$. According to the shape of the two payoff functions
115 $R(x)$ and $L(x)$, defined in the unitary interval $x \in [0, 1]$, several situations can be considered, ranging from the well known
116 n -players prisoner’s dilemma (with e.g. $R(x) > L(x) \forall x \in [0, 1]$ and $R(1) < L(0)$) to minority games (with just one intersection
117 and $R(0) > L(0)$, $R(1) < L(1)$ so that R is dominant with small values of x and dominated with high values) as well as many
118 other cases characterized by several intersections between the two payoff curves, as described in Schelling (1973, 1978) or
119 Granovetter (1978), Granovetter and Soong (1983).

120 Assuming that at each time period $t = 0, 1, \dots$ the payoffs $R(x(t))$ and $L(x(t))$ obtained by agents that belong to both
121 fractions of players are common knowledge, we describe the dynamic adaptive process that describes the time evolution of
122 the number of agents choosing R by using the same kind of exponential replicator dynamics as in Bischi and Merlone (2017),

123 based on the *monotone selection dynamics* proposed in [Cabrales and Sobel \(1992\)](#), see also [Hofbauer and Sigmund \(2003\)](#):

$$124 \quad x(t+1) = f(x(t)) = \frac{x(t) \exp(\alpha R(x(t)))}{x(t) \exp(\alpha R(x(t))) + (1-x(t)) \exp(\alpha L(x(t)))} \quad (1)$$

$$= \frac{x(t)}{x(t) + (1-x(t)) \exp(-\alpha g(x(t)))}$$

124 where the “gain” function

$$125 \quad g(x) = R(x) - L(x) : [0, 1] \rightarrow \mathbb{R} \quad (2)$$

125 has been introduced so that positive values of $g(x)$ cause an increase of the fraction of agents choosing R whereas negative
126 values of g cause an increase of the number of agents choosing L , the intensity of transition at time t to the dominant
127 choice being proportional to $g(x(t))$ through the proportionality coefficient $\alpha > 0$, called “speed of reaction”, a parameter
128 that expresses the propensity to switch to the opposite choice as a consequence of a payoff gain observed at the current
129 time period. This form of discrete-time replicator equation has the crucial property that if $x(0) \in [0, 1]$ then $x(t) \in [0, 1]$ for
130 each $t \geq 0$, as it follows from the evident inequality $0 \leq \frac{x}{x+(1-x)\exp(-\alpha g(x))} \leq 1$.

131 In [Bischi and Merlone \(2017\)](#) this dynamic setup has been applied to the description of minority games, characterized
132 by a unique intersection between the payoff curves and the property that players gain higher payoff when they choose the
133 strategy which is chosen by the minority of players, i.e. $R(x)$ is higher than $L(x)$ when x is small, whereas $R(x)$ is less than
134 $L(x)$ for values of x close to 1. Instead, in this paper we consider the case of two interior intersections describing a situation
135 in which one alternative, e.g. R , is convenient for intermediate values of the fraction x of agents choosing it, whereas the
136 opposite choice L has higher payoff when extreme polarization occurs, both for values of x close to 0 and values close to 1.
137 So, in the following we shall consider payoff functions according to the following assumption.

138 **Assumption on payoff functions.** $R : [0, 1] \rightarrow \mathbb{R}$ and $L : [0, 1] \rightarrow \mathbb{R}$ are differentiable functions such that $R(0) < L(0)$,
139 $R(1) < L(1)$ and $R(x) > L(x)$ if and only if $q^* < x < p^*$ where the two thresholds q^* and p^* are such that $0 < q^* < p^* < 1$, with
140 the transversality condition $R'(q^*) > L'(q^*)$ and $R'(p^*) < L'(p^*)$.

141 2.2. Existence and stability of steady states

142 It is straightforward to see that $x_0^* = 0$ and $x_1^* = 1$, where “all players play L ” and “all players play R ” respectively, are
143 boundary equilibrium points. Moreover, interior equilibria exist at any x^* such that $g(x^*) = 0$, i.e. characterized by iden-
144 tical payoffs $L(x^*) = R(x^*)$. A consequence of the assumption on payoff functions given above is that $R(q^*) = L(q^*)$ and
145 $R(p^*) = L(p^*)$, due to continuity of the payoff functions. Hence the two thresholds are also interior equilibrium points for
146 the dynamic model 1, as $g(q^*) = g(p^*) = 0$, with slopes of the gain function characterized by $g'(q^*) > 0$ and $g'(p^*) < 0$ re-
147 spectively.

148 The following result holds; a proof is given in the Appendix.

149 **Proposition 1.** Under the assumptions on payoff functions stated above, the equilibrium point $x_0^* = 0$ is always locally asymptot-
150 ically stable, the equilibrium points q^* and $x_1^* = 1$ are always unstable, whereas p^* is locally asymptotically stable provided that

$$151 \quad \alpha < \alpha_f = \frac{2}{p^*(1-p^*)g'(p^*)} \quad (3)$$

152 where $g'(p^*) = R'(p^*) - L'(p^*) < 0$ is the slope difference between two payoff curves at p^* . If the parameter α increases across
153 the bifurcation value α_f then p^* becomes unstable through a flip (or period doubling) bifurcation.

154 A typical graph of the payoff curves $R(x)$ and $L(x)$ considered in this paper is shown in the left panel of [Fig. 1](#), and
155 the corresponding graph of the one-dimensional map $f(x)$ defined in (1) is represented in the right panel, with its bimodal
156 shape obtained with suitable values (not too small) of the parameter α , with relative maximum and minimum points at
157 $x_{\max} < x_{\min}$ respectively, and corresponding relative maximum and minimum values $c_{\max} = f(x_{\max}) < c_{\min} = f(x_{\min})$. The
158 particular expressions of the payoff functions used to get this figure, as well as the numerical simulations performed in the
159 following, are given by

$$160 \quad R(x) = ax(1-x), \quad a > 0, \quad L(x) = cx + d \quad (4)$$

160 with parameters $a = 8$, $c = d = 1$. This particular set of parameters is just fixed in order to have two interior intersections,
161 namely $q^* \approx 0.18$ and $p^* \approx 0.69$, and the flip bifurcation of p^* obtained for increasing values of the speed of reaction α occurs
162 at $\alpha_f \approx 2.29$. So, in the dynamic scenario shown in the right panel of [Fig. 1](#), obtained for $\alpha = 2$, two attracting equilibria
163 coexist, x_0^* and p^* , whose basins of attraction $\mathfrak{B}(x_0^*) = (0, q^*)$ and $\mathfrak{B}(p^*) = (q^*, 1)$, represented with different colors along
164 the diagonal in the figure, are contiguous open intervals separated by the unstable equilibrium q^* . If the initial share of
165 population of agents that choose option R is less than the threshold value q^* then the endogenous evolutionary dynamics
166 will lead to the extinction of such fraction, i.e. all agents will choose L in the long run, whereas initial share of agents
167 choosing R above q^* will evolve towards the equilibrium p^* where both options are chosen, each by a positive population
168 fraction.

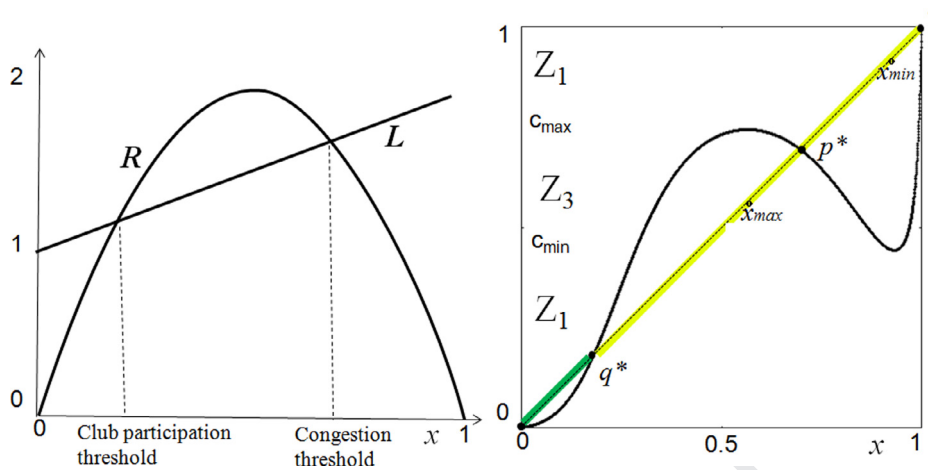


Fig. 1. Left: Payoff functions $R(x)$ and $L(x)$ according to (4) with parameters $a = 8$, $c = d = 1$. Right: graph of the map $f(x)$ defined in (1) with payoff functions (4) and speed of reaction $\alpha = 2$. Different colors along the diagonal represent the basins of attraction of the two stable equilibrium points $x_0^* = 0$ and $p^* = 0.69$.

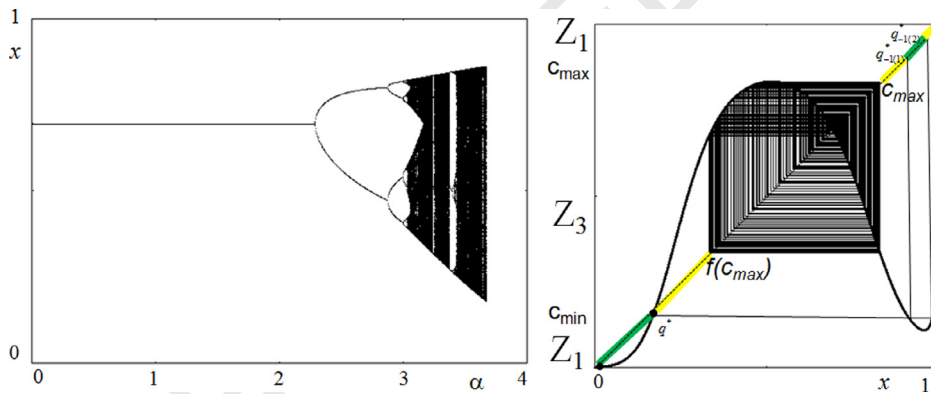


Fig. 2. Left: Bifurcation diagram obtained for increasing values of the speed of reaction α and the same payoff functions as in Fig. 1. Right: graph of the function $f(x)$ with $\alpha = 3.2$ after the contact bifurcation leading to non connected basins.

169 Similar results are also obtained with different choices of functions $R(x)$ and $L(x)$ satisfying the assumptions stated above.
 170 In fact, in any case (even if both $R(x)$ and $L(x)$ are monotonic functions with two interior intersections) the shape of the
 171 function $f(x)$ that governs the dynamic evolution is essentially the same, with critical points x_{min} and x_{max} existing for
 172 sufficiently high values of the speed of reaction α .

173 2.3. Two different kinds of complexity

174 As the speed of reaction α is increased, two routes to dynamic complexity can be observed: one related to the creation
 175 of more complex attractors around p^* , say $A(p^*)$, nested inside the trapping region $[f(c_{max}), c_{max}]$; the other one related to
 176 the creation of complex topological structures of the basins of attraction, which are transformed from connected intervals
 177 into the union of several (even infinitely many) disjoint portions.

178 The first kind of complexity is opened by the flip bifurcation at which p^* loses stability, occurring for increasing values of
 179 α across the local bifurcation value α_f according to proposition 1, leading to the well known period doubling route to chaos.
 180 (see the bifurcation diagram in the left panel of Fig. 2). It is worth noticing that the attractor $A(p^*)$ around the unstable
 181 fixed point p^* , which may be periodic or chaotic, is bounded above by the maximum value c_{max} and below by its image
 182 $f(c_{max})$ (see the right panel of Fig. 2). Indeed, as a matter of fact it is quite evident that if we iterate the map f starting from
 183 any initial condition in the basin $\mathfrak{B}(A(p^*))$, then no values can be obtained above c_{max} , and consequently no values can
 184 be mapped below its image $f(c_{max})$. In other words, interval $[f(c_{max}), c_{max}]$ is trapping, i.e. any trajectory generated from an
 185 initial condition in $\mathfrak{B}(A(p^*))$ enters it after a finite number of iterations and then never goes out of it.

186 However, as it can be seen in the figure, another remarkable (global) bifurcation occurred, causing the transformation
 187 of the basins into a non connected set. The outcome of this second route to complexity is caused by the presence of the
 188 threshold value q^* and the fact that the iterated map f is noninvertible, or “many to one”, i.e. distinct points exist that

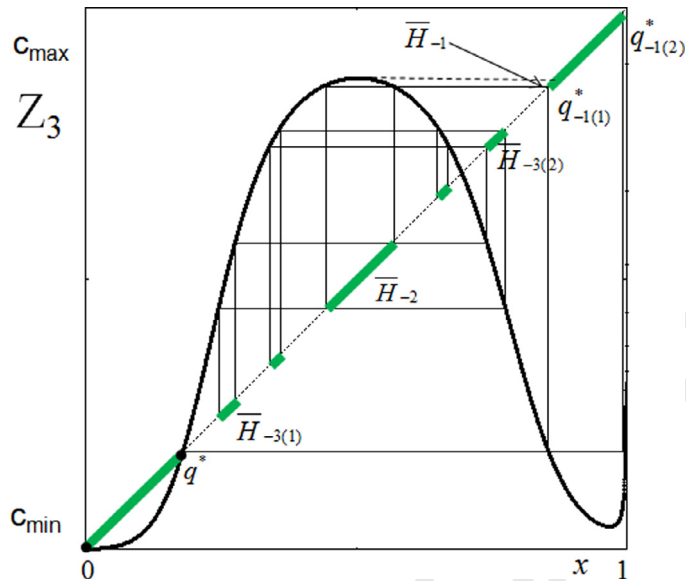


Fig. 3. For $\alpha = 3.8$, just after the final bifurcation occurring at the contact between c_{\max} and the basin boundary $q_{-1(1)}^*$. Main holes of $\mathfrak{B}(x_0^*)$ inside the former trapping interval $[f(c_{\max}), c_{\max}]$.

189 are mapped into the same image, say $x_1 \neq x_2$ such that $f(x_1) = f(x_2)$. This can be equivalently stated by saying that in
 190 the range of the map f there are points with several distinct preimages, so it can be divided into different portions, or
 191 zones, characterized by a different number of preimages. In the particular case of the map f in (1), following the notation
 192 introduced in Mira et al. (1996), we can say that it is a $Z_1 - Z_3 - Z_1$ map, where Z_k denotes the set of points that have k
 193 rank-1 preimages, being $Z_1 = [0, c_{\min}) \cup (c_{\max}, 1]$ and $Z_3 = [c_{\min}, c_{\max}]$.

194 On the basis of this mathematical background, it is now easy to realize that in the situation shown in Fig. 1 the unstable
 195 fixed point $q^* \in Z_1$, hence it has only one preimage given by itself (being it a fixed point, $f(q^*) = q^*$). This is the reason why
 196 it is the unique boundary point that separates the two basins of attraction. This is true as far as $q^* < c_{\min}$. As the parameter
 197 α increases, the minimum value $c_{\min} = f(x_{\min})$ is shifted downwards and when it reaches q^* and crosses it, so that $c_{\min} < q^*$,
 198 then q^* , as well as a portion of $\mathfrak{B}(x_0^*)$, enters Z_3 , as it can be seen in Fig. 2 where $q^* \in Z_3$. This implies that now two more
 199 preimages exist, say $q_{-1(1)}^*$ and $q_{-1(2)}^*$, both belonging to the basin boundary as well (see the right panel of Fig. 2). So, the
 200 contact of the threshold q^* with the critical point c_{\min} marks the occurrence of a global (or contact) bifurcation at which a
 201 portion of $\mathfrak{B}(x_0^*)$, say H_0 , enters Z_3 and its rank-1 preimages form a new disjoint portion of the basin of attraction $\mathfrak{B}(x_0^*)$,
 202 say H_{-1} , nested inside $\mathfrak{B}(A(p^*))$, which consequently becomes a non connected set as well.

203 However this is not the end of the story, as the non connected portion of $\mathfrak{B}(x_0^*)$, given by $H_{-1} = (q_{-1(1)}^*, q_{-1(2)}^*) \in Z_1$,
 204 has further preimages, represented by smaller and smaller portions (really infinitely many, a countable set of preimages of
 205 higher rank) that accumulate in a left neighborhood of the unstable equilibrium $x_1^* = 1$ (not visible in Fig. 2 because too
 206 small).

207 Moreover, as the parameter α increases, the maximum value c_{\max} moves upwards until it has a contact with $\mathfrak{B}(x_0^*)$ at
 208 the point $q_{-1(1)}^*$. This marks another remarkable global bifurcation, at which $q_{-1(1)}^*$ (as well as a portion of H_{-1}) enters
 209 Z_3 so that infinitely many portions of $\mathfrak{B}(x_0^*)$ (preimages of any rank of the portion of $H_{-1} \in Z_3$) are created inside the
 210 former trapping interval $(f(c_{\max}), c_{\max})$ (no longer trapping, of course) and densely distributed inside by the typical process
 211 that reduces the former basin $\mathfrak{B}(A(p^*))$ to a zero measure Cantor set (see Fig. 3 where only the main holes of $\mathfrak{B}(x_0^*)$
 212 are shown). Indeed, after this contact between c_{\max} and the basin boundary, the chaotic attractor $A(p^*)$ is transformed into a
 213 chaotic repeller through a global bifurcation called “final bifurcation” in Mira et al. (1996) (see also Abraham et al. (1997))
 214 or “boundary crisis” in Grebogi et al. (1983). After this bifurcation the only attractor remains $x_0^* = 0$, as it is clearly seen in
 215 the bifurcation diagram shown in the left panel of Fig. 2 for $\alpha > 3.7$ approximately.

216 To sum up, the presence of the threshold point q^* gives rise to the coexistence of two attractors, each with its own basin
 217 of attraction, the threshold being the boundary, or watershed, that separates the two basins. Moreover, the bimodal shape
 218 of the map f that gives the time evolution of the adaptive process defined by the replicator dynamics, together with the
 219 presence of the threshold q^* , for increasing values of the speed of reaction α gives rise to remarkable global bifurcations
 220 leading to the creation of complex topological structures of the basins implying a strong path dependence.

221 In the following we shall investigate the effects, on the dynamic properties of the evolutionary model after the introduc-
 222 tion of memory effects.

223 3. The model with finite memory

224 3.1. Dynamic model setup

225 The evolutionary model proposed in the previous section is based on current payoffs, that is, the players' decisions about
 226 the next period strategy choice are based on the knowledge of current payoffs only. A generalization of this assumption
 227 consists in replacing the current payoff with a weighted average of it and some of the previously observed ones. That is, we
 228 consider a form of memory in the model (1) by assuming that players decide to switch their strategy according to an average
 229 of the payoffs observed during the more recent M time periods (a sort of moving average, see e.g. Chiarella et al. (2006),
 230 see also Bischi and Merlone (2017))

$$230 \quad U_R(t) = \sum_{k=0}^M \omega_k R(t-k); \quad U_L(t) = \sum_{k=0}^M \omega_k L(t-k) \quad (5)$$

231 where M is the length of memory and ω_k are the weights, normalized according to $\sum_{k=0}^M \omega_k = 1$. Of course, for $M = 0$ the
 232 case with no memory is obtained, and for $M > 0$ the distribution of weights can be used to modulate the "shape" of past
 233 memory. The model (1) with (5), given by

$$233 \quad x(t+1) = \frac{x(t)}{x(t) + (1-x(t)) \exp[-\alpha(U_R(t) - U_L(t))]}$$

234 becomes a difference equation of order $M+1$, equivalent to a $M+1$ dimensional discrete dynamical system. In order to
 235 investigate the memory effects and, at the same time, maintain a low dimensionality so that the model is still analytically
 236 tractable, we consider the case $M = 1$ with weights $\omega_0 = \omega$ and $\omega_1 = (1-\omega)$, that is

$$236 \quad \begin{aligned} U_R(t) &= (1-\omega)R(x(t)) + \omega R(x(t-1)) \\ U_L(t) &= (1-\omega)L(x(t)) + \omega L(x(t-1)) \end{aligned} \quad (6)$$

237 where $\omega \in [0, 1]$, so that only the current payoff is considered, for $\omega = 0$, whereas agents only consider the payoff of the
 238 previous period (ignoring the current one) for $\omega = 1$, i.e. a situation of lagged information. An uniform average of the two
 239 payoffs is obtained when $\omega = \frac{1}{2}$, i.e. when considering the arithmetic mean. In the following we shall only consider weights
 240 in the range $\omega \in [0, 0.5]$ in order to get non increasing memory of past states, so that this finite memory case can be
 241 compared with the infinite discounted memory of Section 4.

242 The model can be expressed as a two-dimensional discrete dynamical system after the introduction of the auxiliary
 243 variable $y(t) = x(t-1)$,

$$243 \quad \begin{cases} x(t+1) = \frac{x(t) \exp[\alpha((1-\omega)R(x(t)) + \omega R(y(t)))]}{x(t) \exp[\alpha((1-\omega)R(x(t)) + \omega R(y(t)))] + (1-x(t)) \exp[\alpha((1-\omega)L(x(t)) + \omega L(y(t)))]} \\ y(t+1) = x(t) \end{cases} \quad (7)$$

244 3.2. Existence and stability of steady states

245 It is easy to check that the equilibria are the same as in the model without memory, i.e. $y^* = x^*$ with x^* at the boundaries
 246 $\{0, 1\}$ or at the interior intersections where $R(x^*) = L(x^*)$. However, the stability conditions are influenced by the "memory
 247 parameter" ω , as stated by the following proposition.

248 **Proposition 2.** Let $O^* = (0, 0)$, $Q^* = (q^*, q^*)$, $P^* = (p^*, p^*)$ and $I^* = (1, 1)$ where q^* and p^* are the interior intersections of the
 249 payoff functions $R(x)$ and $L(x)$. Then O^* is a stable node; I^* is an unstable node; Q^* is a saddle point; P^* is locally asymptotically
 250 stable if $\omega_f < \omega < \omega_h$, with

$$250 \quad \omega_f = \frac{1}{2} + \frac{1}{\alpha p^* (1-p^*) g'(p^*)} \quad (8)$$

251 and

$$251 \quad \omega_h = -\frac{1}{\alpha p^* (1-p^*) g'(p^*)} \quad (9)$$

252 where $\omega_f < \omega_h$ provided that

$$252 \quad \alpha x^* (1-x^*) g'(x^*) > -4. \quad (10)$$

253 Under this latter assumption, if the memory parameter ω exits the stability interval $[\omega_f, \omega_h]$ decreasing through the lower
 254 bound ω_f then P^* loses stability through a flip bifurcation. If ω exits the stability interval increasing through the upper bound ω_h
 255 then P^* loses stability through a Neimark-Sacker bifurcation.

A proof of this Proposition is given in the Appendix, where it is worth noticing that, as expected, the condition for the flip bifurcation of P^* , i.e. $P(-1) = 2 + \alpha(1 - 2\omega)p^*(1 - p^*)g'(p^*) = 0$ (see the Appendix) for $\omega = 0$ reduces to the one given in Proposition 1 for the model without memory. Moreover, starting from a value of the speed of reaction α such that $-4 < \alpha p^*(1 - p^*)g'(p^*) < -2$, according to Proposition 2 the equilibrium P^* is stable for intermediate values of the memory parameter ω , i.e. when the weighted average is close to the uniform arithmetic mean, whereas P^* is unstable for the model without memory, according to Proposition 1. Instead, both the asymmetric averages that give too much weight to the current value or to the previous value, generate oscillatory dynamics. A typical bifurcation diagram, obtained with the payoff functions defined in (4) with $a = 8$, $c = d = 1$ and speed of reaction $\alpha = 3$ is shown in the left panel of Fig. 4.

As it can be seen, this bifurcation diagram not only confirms the existence of the stability range analytically computed in Proposition 2, but also provides numerical evidence for the supercritical nature of the two local bifurcations, as a stable oscillation of period 2 is obtained as the memory parameter ω decreases below ω_f , and a stable quasi-periodic motion along a closed invariant curve is observed as ω increases above ω_h . Moreover, a representation of the trajectories, the attractors and the basins of attraction in the phase space $(x, y) \in [0, 1] \times [0, 1]$ clearly show that a unique interior attractor, say $A(P^*)$, exists for this set of parameters.

However, coexistence of several interior attractors can be easily observed with different parameters' constellations. Indeed, the presence of coexisting attractors is not an exception, but rather becomes the rule, when memory is introduced in the model. As coexistence of attractors implies path dependence, agents' memory makes the dynamics more complex, consistent to empirical examples as the ones analyzed in Schreyögg et al. (2011).

3.3. Coexistence of attractors and basins' bifurcations

For $\alpha = 3.7$, the superposition of two bifurcation diagrams shown in the right panel of Fig. 4, one obtained with increasing values of the bifurcation parameter ω and the other one with decreasing values, reveals that in the range of intermediate values of the bifurcation parameter ω , approximately with $\omega \in [0.1906, 0.3093]$, two interior attractors coexist: the stable equilibrium P^* (or a different attractor $A(P^*)$) around it for values of the memory parameter ω outside the stability range $[\omega_f, \omega_h]$ and a stable cycle of period 3. Together with the boundary stable equilibrium O^* this gives rise to a dynamic situation characterized by the coexistence of three attractors, each with its own basin of attraction. Of course, this represents a more complex dynamic scenario, in particular a more complicated distribution of three basins of attraction that share the phase plane, thus determining a more crucial role of initial conditions, that may lead to three different kinds of long run behaviors: convergence to the equilibrium O^* where all players play L , or to the equilibrium P^* with fixed fractions of players playing R and L , or to an oscillatory behaviour (periodic in this case, but slight changes of the parameters can easily transform the latter attractor into a chaotic one). In other words, the presence of memory may stabilize the interior equilibrium P^* but at the same time may give a stronger path dependence.

It is worth noticing that such a coexistence could not be predicted by any analytical local analysis of the dynamical system, and if our analysis were limited to the proof of Proposition 2, together with its immediate numerical confirmation given by the bifurcation diagram in the left panel of Fig. 4, then a quite incomplete, and even misleading, description of the dynamic properties of the evolutionary model considered would be given. Instead, when such multistability is numerically revealed, a study of the basins of attraction of the three coexisting attractors becomes crucial in order to manage path dependence, i.e. how the three attractors share the phase space on which initial conditions are taken.

In order to illustrate the occurrence of global bifurcations leading to complex topological structures of the basins numerical explorations are necessary, guided by the mathematical background on noninvertible maps and critical curves, the two dimensional analogue of critical points already used in the previous section (see the Appendix for a general definition of critical curves and their particular expression for the model analyzed in this paper).

Let us start with a dynamic scenario characterized by the coexistence of two attractors, the equilibrium O^* and the chaotic attractor $A(P^*)$ existing around the equilibrium P^* obtained with the same set of parameters as in the bifurcation diagram in right panel of Figure 4 and memory parameter $\omega = 0.1$. This situation, shown in the left panel of Fig. 5, is similar to the one described for the one-dimensional model without memory, with a simply connected basin of $A(P^*)$ represented by the white region and the basin of O^* represented by the green region. The basin boundary is formed by the stable set of the saddle point Q . The critical curves LC_{-1} and LC are represented as well, whose analytical expression is given in the Appendix. LC divides the phase plane into regions Z_1 and Z_3 whose points have one or three rank-1 preimages respectively. As it can be seen in the figure, a segment of LC is close to a contact with the right boundary of the basin $\mathfrak{B}(O^*)$. Indeed, this contact occurs for increasing values of the speed of reaction α , as shown in the central panel of Fig. 5 obtained with $\alpha = 3.9$. At this stage the attractor $A(P^*)$ is a cycle of period 4, a "periodic window", but this has no influence on the global bifurcation: After the contact a new portion H_0 of the basin $\mathfrak{B}(O^*)$ enters Z_3 and the two extra preimages, located at opposite sides of LC_{-1} and merging along it, form a hole of $\mathfrak{B}(O^*)$ nested inside $\mathfrak{B}(A(P^*))$, denoted by H_{-1} in the figure. The mechanism leading to non connected basins is essentially the same as the one analyzed in Fig. 2 for the model without memory. Other non connected portions exist, preimages of higher rank of H_0 , but they are not visible in the figure (one can be seen in the right panel). Also the final bifurcation, at which the attractor $A(P^*)$ is transformed into a chaotic repeller, occurs for higher values of α , like in the one-dimensional model without memory. The contact that marks the occurrence of such global bifurcation is shown in the right panel of Fig. 5, obtained for $\alpha = 3.96$.

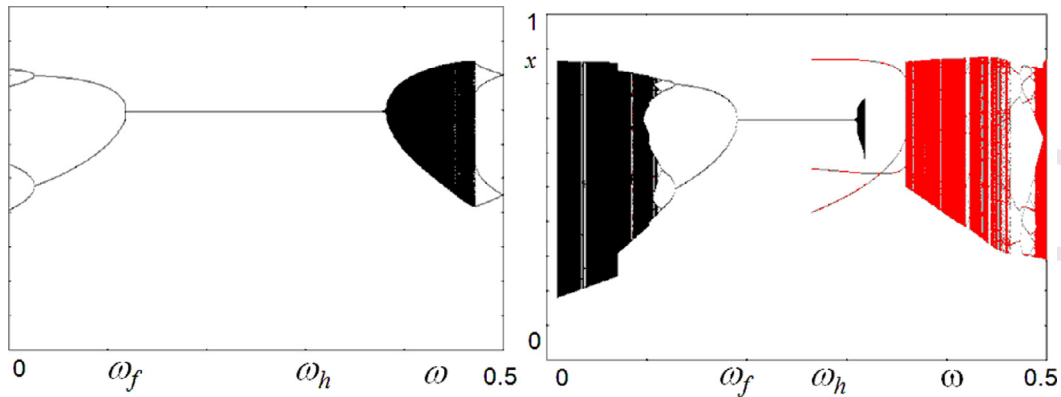


Fig. 4. Model with finite memory (7). Left: Bifurcation diagram obtained for increasing values of the memory parameter ω and other parameters fixed at the values $a = 8$, $c = d = 1$, $\alpha = 3$. Right: For $\alpha = 3.7$ and other parameters as in the left panel, superposition of two bifurcation diagrams, one obtained with increasing values and the other one with decreasing values of the bifurcation parameter ω , each trajectory being obtained by taking the last iterated point of the previous one as initial condition.

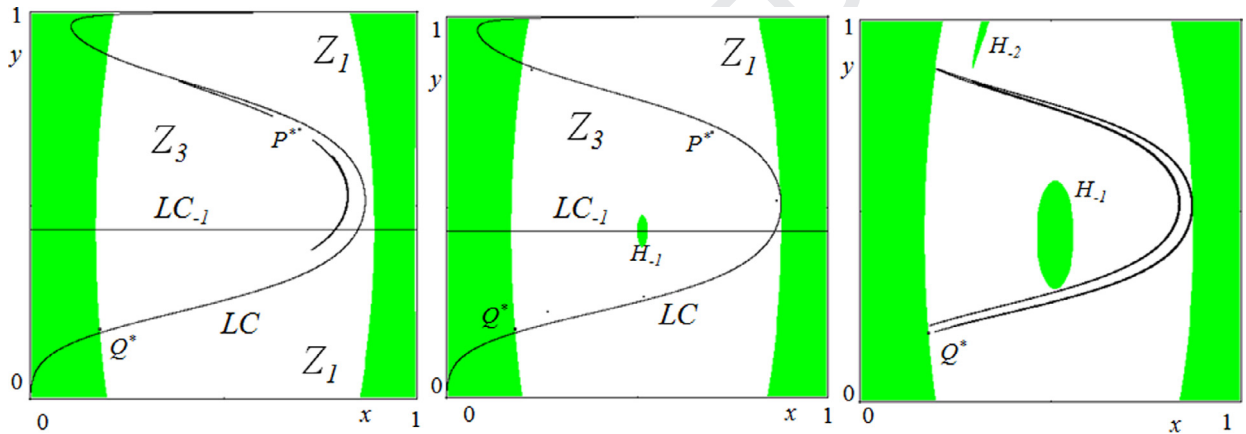


Fig. 5. Attractors and basins in the phase space of the model with finite memory (7). Left: With the same set of parameters as in the right panel of Fig. 4 and memory parameter $\omega = 0.1$. Critical curves LC and LC_{-1} are represented as well. Center: $\alpha = 3.9$. Right: $\alpha = 3.96$.

314 Similar contact bifurcations can be detected even in the case of three coexisting attractors, as it can be seen in the
 315 sequence of dynamic situations shown in Fig. 6. The three figures are obtained with the same set of parameters as in the
 316 bifurcation diagram of the right panel of Fig. 4 and different values of the memory parameter ω in the range of coexistence
 317 of three attractors. In the left panel, where $\omega = 0.23$, the equilibrium P^* is a stable focus, whose basin of attraction $\mathfrak{B}(P^*)$
 318 is represented by the yellow region, a stable cycle of period 3, say C_3 , attracts the initial condition taken in $\mathfrak{B}(C_3)$ represented
 319 by the red region and, finally, the usual stable equilibrium O^* exists, whose basin $\mathfrak{B}(O^*)$ is represented by the green region.
 320 In this dynamic scenario two segments of LC are close to basin boundaries: a contact between LC and $\mathfrak{B}(O^*)$ in the upper-
 321 left part of the figure and a possible contact between LC and $\mathfrak{B}(C_3)$ indicated by the arrow. The effects of these two contacts
 322 are shown in the central panel of Fig. 6, obtained with $\omega = 0.25$: After the portion of $\mathfrak{B}(O^*)$ exits Z_1 to stay in Z_3 the strip of
 323 $\mathfrak{B}(O^*)$ on the right becomes disconnected, formed by two non connected tongues. As far as the other contact is concerned,
 324 a portion (say K_0) of $\mathfrak{B}(C_3)$ enters Z_3 and as a consequence new non connected portions of $\mathfrak{B}(C_3)$ are created on the left.
 325 Moreover, another contact is going to occur between LC and the central portion of $\mathfrak{B}(C_3)$. The right panel of the figure,
 326 obtained with $\omega = 0.27$, reveals that such contact occurs, after which a portion of $\mathfrak{B}(C_3)$ passes from Z_3 to Z_1 thus causing
 327 the merging of the two holes of $\mathfrak{B}(C_3)$ on the left that are transformed from two non-connected holes into a unique hole
 328 of $\mathfrak{B}(C_3)$ inside $\mathfrak{B}(P^*)$.

329 To sum up, without further entering the details on global bifurcation of the basins of attraction (we refer the reader to
 330 Gumowski and Mira, 1980; Mira et al., 1996; Abraham et al., 1997; Agliari et al., 2002 for a deeper view) we can conclude
 331 that generally any contact between LC and a basin boundary causes a qualitative change in the topological structure of the
 332 basins. As a last example we show in Fig. 7 the effect of a contact of LC and the boundary of $\mathfrak{B}(P^*)$ occurring with $\alpha = 4$
 333 and $\omega = 0.26$, leading to the creation of a small hole of $\mathfrak{B}(P^*)$ nested inside $\mathfrak{B}(C_3)$.

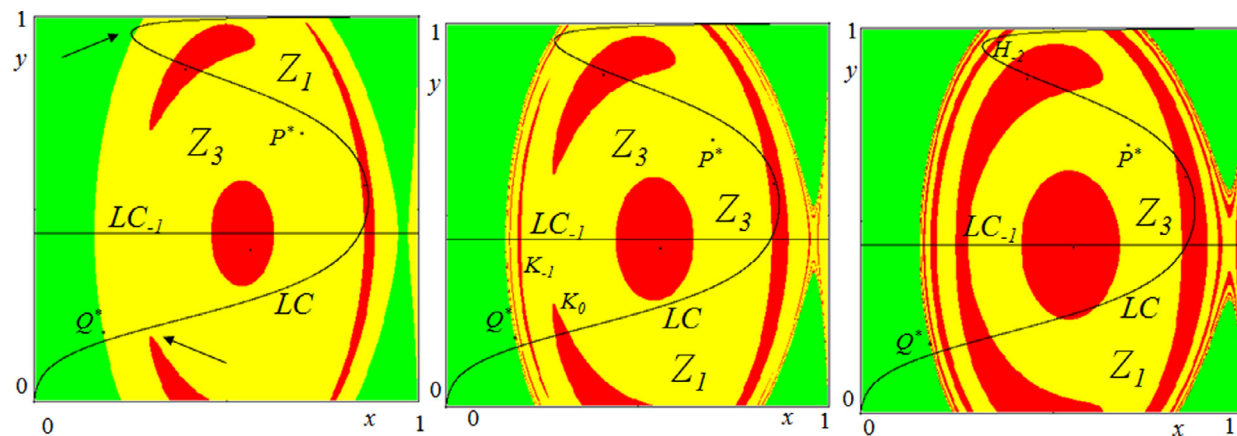


Fig. 6. Attractors and basins of attraction, represented by different colors, for the model with finite memory (7). All the parameters are the same as in the bifurcation diagram of the right panel of Fig. 4 and different values of the memory parameter ω are taken in the range of coexistence of three attractors. Left: $\omega = 0.23$. Center: $\omega = 0.25$. Right: $\omega = 0.27$.

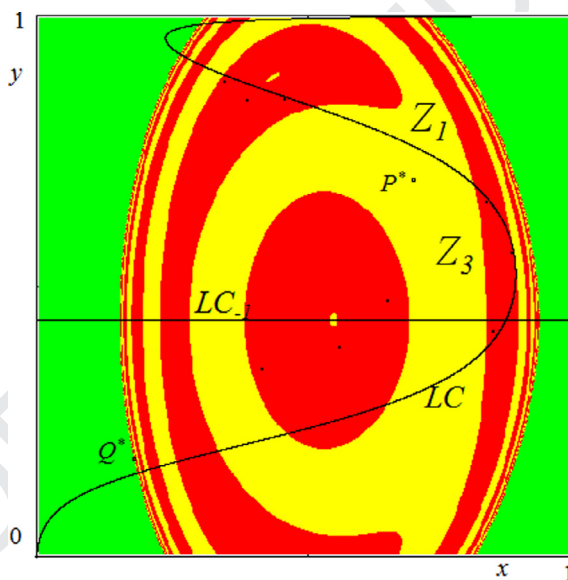


Fig. 7. Attractors and basins for the model (7) with $a = 8$, $c = d = 1$, $\alpha = 4$, $\omega = 0.26$.

334 It is also worth remarking that we have not observed a so severe path dependence in the evolutionary model (1) without
 335 memory, where at most two coexisting attractors have been evidenced. We stress again that such dynamic scenarios, to-
 336 gether with their economic consequences, clearly show the importance of a global analysis of nonlinear dynamical systems,
 337 which can often be performed only through by combining analytical, geometrical and numerical methods.

338 **4. Infinite discounted memory**

339 The introduction of a finite memory of order greater than one, i.e. the inclusion of other previous states in the informa-
 340 tion set used to compute the fitness measure considered in the replicator dynamics, gives rise to higher dimensional dynam-
 341 ical systems which are difficult to be mathematically analyzed by analytical methods. Instead, following Dindo (2005) and
 342 Bischi and Merlone (2017), we can introduce in the evolutionary model (1) a form of memory that includes the previous
 343 states by considering a fitness measure given by a discounted sum of all the payoffs gained along the whole story of the
 344 repeated binary choice game. This is obtained by taking, at each time step, a convex combination of the current payoff and
 the fitness measure observed in the previous time period:

$$\begin{aligned}
 U_R(t) &= (1 - \omega)R(t) + \omega U_R(t - 1) \\
 U_L(t) &= (1 - \omega)L(t) + \omega U_L(t - 1)
 \end{aligned}
 \tag{11}$$

346 with $\omega \in [0, 1]$, $U_R(0) = U_L(0) = 0$. By backward induction reasoning it is easy to get

$$U_R(t) = (1 - \omega) \sum_{k=0}^{t-1} \omega^k R(t - k) + \omega^t U_R(0)$$

$$U_L(t) = (1 - \omega) \sum_{k=0}^{t-1} \omega^k L(t - k) + \omega^t U_L(0)$$

347 which gives the discounted measure of fitness as a weighted sum with exponentially fading weights. Again, the parameter
348 $\omega \in [0, 1]$ gives a measure of the memory, as $U_i(t) = R(t)$ for $\omega = 0$, whereas the uniform arithmetic mean of all the payoffs
349 observed in the past is obtained in the other limiting case $\omega = 1$. Following Bischi and Merlone (2017), if the recursive
350 scheme (11) is plugged into the evolutionary model (1) then we get

$$x(t+1) = \frac{x(t)}{x(t) + (1 - x(t)) \exp(-\alpha(U_R(t) - U_L(t)))}$$

$$U_R(t+1) = (1 - \omega)R(x(t+1)) + \omega U_R(t)$$

$$U_L(t+1) = (1 - \omega)L(x(t+1)) + \omega U_L(t) \quad (12)$$

351 and subtracting the third equation from the seconds we get

$$x(t+1) = \frac{x(t)}{x(t) + (1 - x(t)) \exp(-\alpha \Delta U(t))}$$

$$\Delta U(t+1) = (1 - \omega)g(x(t+1)) + \omega \Delta U(t) \quad (13)$$

352 where $g(x)$ is given by (2) and $\Delta U(t) = U_R(t) - U_L(t)$. So, despite the long memory represented, the model reduces to an
353 equivalent 2-dimensional map. The fixed points of this map are given by $E_0 = (0, g(0))$, $E_1 = (1, g(1))$, $E_q = (q^*, 0)$ and
354 $E_p = (p^*, 0)$ where q^* and p^* are the usual interior thresholds at which $R(x) = L(x)$.

355 The following proposition, that should be compared with Propositions 1 and 2, gives the local stability properties of the
356 equilibrium points under the assumption of infinite weighted memory.

357 **Proposition 3.** *If the interior equilibrium p^* is stable under the model without memory (1), i.e. $\alpha < \alpha_f$, then it is also stable*
358 *under the model with memory (13), whereas if the p^* is unstable under the model without memory (1), i.e. $\alpha > \alpha_f$, then it*
359 *becomes stable under the model with memory (13) provided that*

$$\omega > \omega_s = \frac{\alpha p^* (1 - p^*) g'(p^*) + 2}{\alpha p^* (1 - p^*) g'(p^*) - 2} \quad (14)$$

360 Moreover, E_0 is always locally asymptotically stable (a stable node); E_1 and E_q are always saddle points.

361 It is worth noticing that, again, an increase of the memory parameter ω has a stabilizing effect because if the equi-
362 librium p^* is stable under the evolutionary dynamics without memory then it remains stable with memory, whereas p^*
363 unstable under the evolutionary dynamics without memory may become stable with a sufficiently strong memory. The
364 stability threshold ω_s is an increasing function of α with $\omega_s(\alpha_f) = 0$ and $\lim_{\alpha \rightarrow \infty} \omega_s = 1$.

365 A typical bifurcation diagram for increasing values of the memory parameter ω is shown in the left panel of Fig. 8,
366 obtained with the same payoff functions used in all the previous numerical simulations and $\alpha = 3.5$. According to
367 Proposition 3, for $\omega > \omega_s \simeq 0.209$, the equilibrium E_p is locally asymptotically stable. For smaller values of the memory pa-
368 rameter ω oscillations around p^* are obtained (periodic or chaotic) with decreasing amplitude as the memory strength
369 increases until the equilibrium becomes stable through a supercritical flip bifurcation. The bifurcation diagram shown in the
370 left panel of Fig. 8 also reveals that for low values of the memory parameter a cases of multistability with three coexisting
371 attractors occurs.

372 We do not investigate further such dynamic scenarios with details on the global dynamic properties necessary to analyze
373 the structure of the basins of attraction, as such analysis essentially requires the same mathematical methods as those
374 illustrated in the previous section, hence we leave such exercise to the reader.

375 We just show in Fig. 8 a typical dynamic scenario of the dynamic model (13) with $a = 8$, $c = d = 1$, $\alpha = 3.5$, $\omega = 0.04$, in
376 a situation where three attractors coexist, namely E_0 , with basin represented by the green region as usual, a chaotic attractor
377 created after the period doubling route of E_p , whose basin is represented by the white region, and a periodic cycle of period
378 3 with red basin.

379 5. Conclusions

380 In this paper we have considered a dynamic binary choice game with several equilibrium points, driven by a replicator
381 evolutionary mechanism, to study the different kinds of long run behaviors of a population of players facing two pure
382 strategies that can be seen as joining or not a club in the presence of cost sharing. This implies that players can enjoy a club
383 good or service provided that a given “participation” threshold is reached. An higher “congestion” threshold is considered as

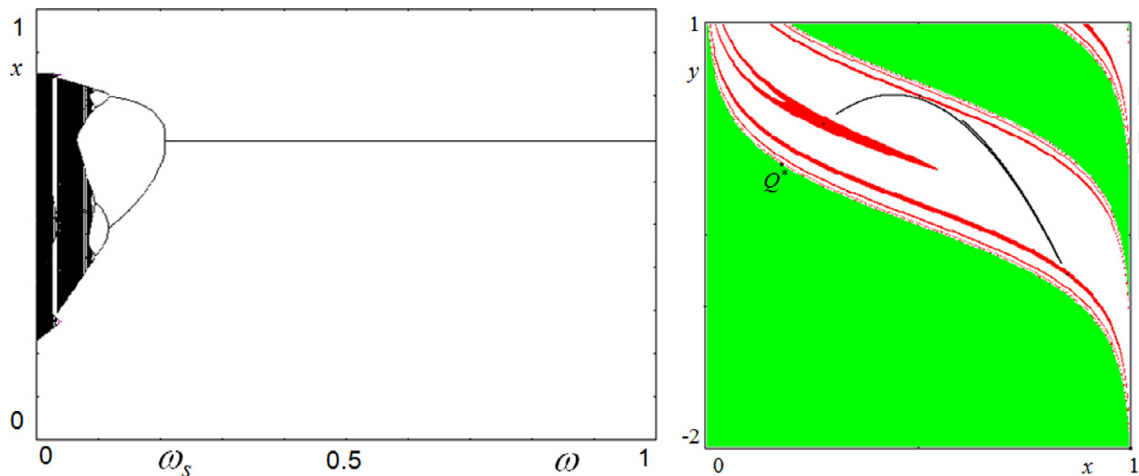


Fig. 8. Left: bifurcation diagram for the model with infinite memory (13) with $a = 8$, $c = d = 1$, $\alpha = 3.5$ and memory parameter ω as bifurcation parameter. Right: Attractors and basins for the model (13) with $a = 8$, $c = d = 1$, $\alpha = 3.5$, $\omega = 0.04$.

well, similar to the one which characterizes minority games. Moreover, the presence of memory effects is also considered, represented by weighted averages of past states on the fitness measure on which the replicator equation is based. So, the model proposed in this paper can be seen as an extension of the minority game considered in Bischi and Merlone (2017) by the introduction of the lower “participation” threshold, an unstable equilibrium that implies the stability of the pure strategy “nobody choosing to join the club”. Moreover, the map that governs the dynamics is S-shaped around the “participation” threshold (see Figs. 1–3). This reflects a dynamic behaviour which is consistent with increasing returns, related to decreasing participation costs (see e.g. Arthur, 1994; Liebowitz and Margolis, 1995; Pierson, 2000) because an upward sloping means that if more players join the club then joining it becomes more attractive. As it is well known, such a dynamic situation implies path dependence. In other words, when several attractors coexist (that may be stable steady states or more complex invariant sets, such as periodic cycles or chaotic sets) the attractor reached in the long run (i.e. the kind of asymptotic evolution) crucially depends on the initial condition. So, the study of the model proposed in this paper reveals two kinds of complexity, one related to complex attracting sets and the other one to the complex structure of the basins of attraction. In particular, the presence of the lower “participation” threshold that causes the stability of the “no participation” equilibrium is also responsible for the global bifurcations leading to complicated topological structures of its basin of attraction. Instead, the presence of the “congestion” threshold may lead to the creation of complex attractors, characterized by oscillations (periodic, quasi-periodic or chaotic) due to overshooting and over-reaction phenomena.

The former kind of complexity has been observed in many social and economic systems. For example, Arthur (1989) and Liebowitz and Margolis (1995) underline the presence of severe path dependence in the adoption of new technologies, a situation that can be described in terms of joining the club of adopters of a given technology, where the two thresholds are related, respectively, to increasing returns for early adopters and congestion effects when the technology saturates the market. Another clear description of path dependence in real world situations similar to the one modelled in this paper is given in Schreyögg et al. (2011), where a case from the German publishing industry is studied, given by the book club division of Bertelsmann AG, that became path-dependent and, finally, locked-in. Several other examples of weak and strong path dependence are given in Pierson (2000), both in economics and politics (e.g. in the location of production in space, environmental protection, technology adoption and national defence), together with a clear qualitative explanation of the underlying mechanisms. In particular, a weaker path-dependence is associated with deterministic chaos, due to sensitive dependence of time evolution on initial conditions, and a strong path dependence associated with quite different long run situations emerging from slight changes of initial conditions. In other words, the two kinds of dynamic complexity studied in this paper. Of course, a deep understanding of the mathematical properties leading to these two kinds of complexity in a simple binary choice model, like the one considered in this paper, may help researchers and decision makers to better understand the basic mechanisms leading to path dependence and consequently to simulate the effects of possible policies to manage it.

The evolutionary binary-choice model proposed in this paper, characterized by the presence of several stable equilibria (as well as other kinds of attractors) is very general, and according to the different application considered one kind of long run evolution may be economically or socially desirable. Under such conditions, the possibility of a detailed analysis of the basins of attraction of the model, as well as the global bifurcations leading to the creation of non-connected basins, may suggest a more proper calibration of the parameters, and related policy implications, in order to avoid these bifurcations that makes forecastings about long run equilibrium selection more difficult.

Both kinds of complexity described above are consequences of the discrete time scale considered in the model, following the explicit suggestions given by Schelling (1973, 1978), see also the discussion on this point in Bischi and Merlone (2009).

424 However, the complex topological structure of the basins is only observed when the map whose iteration gives the dynamic
 425 evolution of the simulated binary game is a noninvertible map (as always occurs in the case of discrete-time replicator
 426 dynamics with several equilibrium points). The study of this kind of dynamical systems requires global methods involving
 427 the concepts of critical sets, as described in Mira et al. (1996), see also Agliari et al. (2002).

428 By using the method of critical curves we have shown peculiar global bifurcations that cause the transition from simple
 429 to complex topological structures of the basins. In particular, the creation of non-connected basins of attraction, with dis-
 430 joint components that are quite far from the corresponding attractor, introduces a counterintuitive effect if compared with
 431 the concept of “corridor stability” often used to describe the effects of multistability and path dependence in economic
 432 problems. This stream of literature, see e.g. Leijonhufvud (1973) or Dohtani et al. (2007), stresses the fact that nonlinear dy-
 433 namic models may have the property that small perturbations are recovered as far as they are confined inside the basin of
 434 attraction of a locally stable equilibrium, whereas larger perturbations lead to time evolutions that further depart from the
 435 equilibrium and go to the coexisting attractor in the long run, a situation that has been called “corridor stability”. Instead,
 436 the results given in this paper show a quite different situation when non-connected basins of attraction, formed by disjoint
 437 (and sometimes far) portions of the basin, exist. In fact, the presence of non-connected basins can be described by saying
 438 that a small perturbation can be recovered by the endogenous dynamics of the evolutive model, a medium-size perturbation
 439 may lead to a different attractor, i.e., a different long run evolution, whereas a larger perturbation may be recovered leading
 440 back the system to the original attractor.

441 Of course, the global dynamic methods used to reveal and explain such dynamic scenarios, together with their economic
 442 consequences, clearly show the importance of a global analysis of nonlinear dynamical systems, which can often be per-
 443 formed only through an heuristic methods obtained by a combination of analytical, geometrical and numerical methods.
 444 And even if the results of this paper are obtained for a particular dynamic model, the mathematical methods used to obtain
 445 these results are quite general.

446 As the effect of memory on binary choice games is concerned, following the approach suggested in Dindo (2005) and
 447 Bischi and Merlone (2017), we have proposed some tractable low-dimensional discrete dynamical system, based on expo-
 448 nential replicator dynamics, in order to describe the time evolution of an economic or social system characterized by the
 449 interaction of a large number of agents who are facing binary choices. In particular we used such a framework to analyze
 450 the effects of memory on the long run outcomes of a repeatedly played binary game, with two kinds of memory. The first
 451 one –which is more innovative– considers only two states and, in some broad sense, is more similar to the finite states
 452 memory considered in Cavagna (1999) and Challet and Marsili (2000), while the second is similar to the one presented in
 453 Dindo (2005). The results of our analysis confirm the stabilizing effects when an uniform memory is introduced, however
 454 an unexpected effect of memory has been stressed, related to the creation of more simultaneous attracting sets, i.e. a more
 455 severe case of multistability with respect to the model without memory. This result has consequences which go beyond the
 456 specific model we were considering. In fact, it shows once more that when considering nonlinear systems both local and
 457 global analysis are necessary to have better understanding of the system. Indeed, our numerical simulations provide further
 458 insight into nonlinear phenomena and the related effects of the presence of memory.

459 In particular, the model studied in this paper gives us the opportunity to learn an important lesson, because in some
 460 ranges on the parameters such that the equilibrium is locally stable, coexisting periodic and chaotic attractors have been
 461 numerically observed, thus giving a strong path dependence. These dynamic scenarios clearly show the importance of a
 462 global analysis of nonlinear dynamical systems, as it was suggested by Chiarella (1990), because a study limited to local
 463 stability and bifurcations, based on the linear approximation of the model around the equilibrium points, sometimes may
 464 be quite incomplete and even misleading.

465 **Compliance with ethical standards.** The authors declare that they have no conflict of interest.

466 Acknowledgments

467 This work has been performed within the framework of COST Action IS1104 “The EU in the new economic complex ge-
 468 ography: models, tools and policy evaluation”, in the framework of the research project on “Dynamic Models for behavioural
 469 economics” financed by DESP-University of Urbino and under the auspices of GNFM (Italy).

470 Appendix A. Proofs of propositions and other mathematical stuff

471 **Proof of Proposition 1.** The first derivative of the map f defined in (1) is

$$f'(x) = \frac{\exp(-\alpha g(x)) [1 + \alpha x(1-x)g'(x)]}{[x + (1-x)\exp(\alpha g(x))]^2} \quad (15)$$

472 From the assumption on the payoff functions we have: $f'(0) = \exp(\alpha g(0)) \in (0, 1)$ as $g(0) = R(0) - L(0) < 0$, hence x_0^*
 473 is stable; $f'(1) = \exp(-\alpha g(1)) > 1$ as $g(1) = R(1) - L(1) < 0$, hence x_1^* is unstable; being $g(q^*) = 0$ we get $f'(q^*) = 1 +$
 474 $\alpha q^*(1 - q^*)g'(q^*) > 1$ being $g'(q^*)$, hence also q^* is an unstable equilibrium. Finally, from $f'(p^*) = 1 + \alpha p^*(1 - p^*)g'(p^*)$
 475 the stability condition $-1 < f'(p^*) < 1$ is always satisfied on the right and is also satisfied on the left provided that
 476 $\alpha p^*(1 - p^*)g'(p^*) > -2$, equivalent to $\alpha < -\frac{2}{p^*(1-p^*)g'(p^*)}$ being $g'(p^*) < 0$. □

477 **Proof of Proposition 2.** The Jacobian matrix of (7) is given by

$$J(x, y) = \begin{bmatrix} \frac{\exp(-\alpha(\cdot)) [1 + \alpha(1 - \omega)x(1 - x)g'(x)]}{[x + (1 - x) \exp(-\alpha(\cdot))]^2} & \frac{\exp(-\alpha(\cdot)) [\alpha\omega x(1 - x)g'(y)]}{[x + (1 - x) \exp(-\alpha(\cdot))]^2} \\ 1 & 0 \end{bmatrix}$$

478 where $(\cdot) = (1 - \omega)g(x) + \omega g(y)$, and since the fixed points are located on the diagonal $y = x$ the expression (\cdot) becomes
479 $(\cdot) = g(x)$ at any equilibrium point. When computed at the equilibrium O^* it becomes

$$J(0, 0) = \begin{bmatrix} \exp(\alpha g(0)) & 0 \\ 1 & 0 \end{bmatrix} \tag{16}$$

480 whose eigenvalues are $z_1 = \exp(\alpha g(0)) \in (0, 1)$ as $g(0) < 0$ and $z_2 = 0$. Hence O^* is a stable node. Analogously

$$J(1, 1) = \begin{bmatrix} \exp(-\alpha g(1)) & 0 \\ 1 & 0 \end{bmatrix} \tag{17}$$

481 whose eigenvalues are $z_1 = e^{-\alpha g(1)} > 1$ as $g(1) < 0$ and $z_2 = 0$, hence I^* is a saddle point.

482 Concerning Q^* from

$$J(Q^*) = \begin{bmatrix} 1 + \alpha(1 - \omega)q^*(1 - q^*)g'(q^*) & \alpha\omega q^*(1 - q^*)g'(q^*) \\ 1 & 0 \end{bmatrix} \tag{18}$$

483 we get the characteristic equation $P(z) = z^2 - Tr \cdot z + Det = 0$ with $Tr = 1 + \alpha(1 - \omega)q^*(1 - q^*)g'(q^*)$ and $Det =$
484 $-\alpha\omega q^*(1 - q^*)g'(q^*)$, from which the Schur (or Jury's) stability conditions (see e.g. Gandolfo, 2010; Elaydi, 1995; Medio and
485 Lines, 2001) become

$$\begin{aligned} P(1) &= 1 - Tr + Det = -\alpha q^*(1 - q^*)g'(q^*) > 0 \\ P(-1) &= 1 + Tr + Det = 2 + \alpha q^*(1 - q^*)g'(q^*)(1 - 2\omega) > 0 \\ 1 - Det &= 1 + \alpha\omega q^*(1 - q^*)g'(q^*) > 0 \end{aligned} \tag{19}$$

486 hence the first one is never verified and the third one is always verified, from which Q^* is a saddle point.

487 Finally, at the equilibrium P^* the Jacobian matrix becomes

$$J(p^*, p^*) = \begin{bmatrix} 1 + \alpha(1 - \omega)p^*(1 - p^*)g'(p^*) & \alpha\omega p^*(1 - p^*)g'(p^*) \\ 1 & 0 \end{bmatrix} \tag{20}$$

488 and following the same arguments with $Tr = 1 + \alpha(1 - \omega)p^*(1 - p^*)g'(p^*)$ and $Det = -\alpha\omega p^*(1 - p^*)g'(p^*)$ we get the fol-
489 lowing sufficient conditions for the local asymptotic stability of P : $P(1) = -\alpha x^*(1 - x^*)g'(x^*) > 0$ for each set of parameters,
490 $P(-1) > 0$ for $\omega > \frac{2 + \alpha x^*(1 - x^*)g'(x^*)}{2\alpha x^*(1 - x^*)g'(x^*)} = \omega_f$ and $1 - Det(E) > 0$ for $\omega < \frac{1}{\alpha x^*(1 - x^*)g'(x^*)} = \omega_h$, where the condition (10) ensures
491 that $\omega_f < \omega_h$, so that the stability range is not empty. The value of ω at which $P(-1)$ becomes negative represent a flip (or
492 period doubling) bifurcation value at which an eigenvalue exits the unit circle through the value -1 , and the one at which
493 becomes negative represents a Neimark-Sacker bifurcation at which a couple of complex and conjugate eigenvalues exit the
494 unit circle of the complex plane (see e.g. Guckenheimer and Holmes, 1983 or Lorenz, 1993). \square

495 **Proof of proposition 3.** Let us rename, just for simplifying notations, $\Delta U(t) = y(t)$. Then the map (13) becomes

$$\begin{aligned} x(t+1) &= \frac{x(t)}{x(t) + (1 - x(t)) \exp(-\alpha y(t))} \\ y(t+1) &= (1 - \omega)g\left(\frac{x(t)}{x(t) + (1 - x(t)) \exp(-\alpha y(t))}\right) + \omega y(t) \end{aligned} \tag{21}$$

496 The Jacobian matrix is

$$J(x, y) = \begin{bmatrix} \frac{e^{-\alpha y}}{(x + (1 - x) \exp(-\alpha y))^2} & \frac{\alpha x(1 - x) \exp(-\alpha y)}{(x + (1 - x) \exp(-\alpha y))^2} \\ (1 - \omega)g'(\cdot) \frac{d(\cdot)}{dx} & (1 - \omega)g'(\cdot) \frac{d(\cdot)}{dy} + \omega \end{bmatrix} \tag{22}$$

497 where $(\cdot) = \frac{x(t)}{x(t) + (1 - x(t)) \exp(-\alpha y(t))}$, so that $\frac{d(\cdot)}{dx} = \frac{\exp(-\alpha y)}{(x + (1 - x) \exp(-\alpha y))^2}$ and $\frac{d(\cdot)}{dy} = \frac{\alpha x(1 - x) \exp(-\alpha y)}{(x + (1 - x) \exp(-\alpha y))^2}$.

498 At the equilibrium E_p it becomes

$$J(E_p) = \begin{bmatrix} 1 & \alpha p^*(1 - p^*) \\ (1 - \omega)g'(p^*) & \alpha(1 - \omega)p^*(1 - p^*)g'(p^*) + \omega \end{bmatrix} \tag{23}$$

499 hence $Tr = 1 + \alpha(1 - \omega)p^*(1 - p^*)g'(p^*) + \omega$ and $Det = \omega$ are, respectively, the trace and the determinant of the matrix
500 (23). The sufficient conditions for the stability of E_p become $P(1) = -\alpha(1 - \omega)p^*(1 - p^*)g'(p^*) > 0$ and $1 - Det = 1 - \omega >$

501 0 for each set of parameters with $\omega \in [0, 1)$, whereas the condition $P(-1) > 0$ becomes $2 + \omega(2 - \alpha p^*(1 - p^*)g'(p^*)) +$
 502 $\alpha p^*(1 - p^*)g'(p^*) > 0$, from which (14) follows. The value of ω at which $P(-1)$ becomes negative represent a flip (or period
 503 doubling) bifurcation value.

504 At the other equilibrium points the stability conditions are quite trivial. In fact

$$\mathbf{J}(E_0) = \begin{bmatrix} \exp(\alpha g(0)) & 0 \\ (1 - \omega)g'(0) \exp(\alpha g(0)) & \omega \end{bmatrix}$$

505 hence both eigenvalues are real and included in the stability range being $\omega \in [0, 1)$ and $g(0) < 0$.

$$\mathbf{J}(E_1) = \begin{bmatrix} [c]cc \exp(-\alpha g(1)) & 0 \\ (1 - \omega)g'(0) \exp(\alpha g(0)) & \omega \end{bmatrix}$$

506 hence E_1 is a saddle being $g(1) < 0$.

$$\mathbf{J}(E_q) = \begin{bmatrix} [c]cc1 & \alpha q^*(1 - q^*) \\ (1 - \omega)g'(q^*) & \alpha(1 - \omega)q^*(1 - q^*)g'(q^*) + \omega \end{bmatrix}$$

507 hence the stability condition $P(1) = -\alpha(1 - \omega)q^*(1 - q^*)g'(q^*) > 0$ is never satisfied being $g'(q^*) > 0$. □

508 **Critical curves**

509 Given a two-dimensional map $T: (x, y) \rightarrow (x', y')$, the point $(x', y') \in \mathbb{R}^2$ is called rank-1 image under T of the point
 510 $(x, y) \in S \subseteq \mathbb{R}^2$. A map is noninvertible if it is “many-to-one”, that is, distinct points may have the same image. Geometrically,
 511 the action of a noninvertible map can be expressed by saying that it “folds and pleats” S , so that distinct points are mapped
 512 into the same point. This is equivalently stated by saying that several inverses are defined in some points of S , and these
 513 inverses “unfold” S .

514 For a noninvertible map, S can be subdivided into regions Z_k , whose points have k distinct rank-1 preimages. Gener-
 515 ally, for a continuous map, as the point (x', y') varies, pairs of preimages appear or disappear as it crosses the boundaries
 516 separating different regions. Hence, such boundaries are characterized by the presence of at least two coincident (merging)
 517 preimages. This leads us to the definition of *critical curves*, one of the distinguishing features of noninvertible maps. The
 518 critical curve of rank-1, denoted by LC (from the French “Ligne Critique”) is defined as the locus of points having two, or
 519 more, coincident rank-1 preimages. These preimages are located in a set called critical curve of rank-0, denoted by LC_{-1} .
 520 The curve LC is the two-dimensional generalization of the notion of critical value (local minimum or maximum value) of a
 521 one-dimensional map, and LC_{-1} is the generalization of the notion of critical point (local extremum point). As in the case
 522 of differentiable one-dimensional maps, where the derivative necessarily vanishes at the local extremum points, for a two-
 523 dimensional continuously differentiable map the set LC_{-1} belongs to the set of points in which the Jacobian determinant
 524 vanishes

$$LC_{-1} \subseteq \{x \in \mathbb{R}^2 : \text{Det}(\mathbf{J}(x)) = 0\}$$

525 and LC is the image of LC_{-1} , i.e., $LC = T(LC_{-1})$. In the case of the map (7) the Jacobian matrix is

$$\mathbf{J}(\mathbf{x}) = \begin{bmatrix} \frac{\exp(-\alpha(\cdot)) [1 + \alpha(1 - \omega)x(1 - x)G'(x)]}{[x + (1 - x) \exp(-\alpha(\cdot))]^2} & \frac{\exp(-\alpha(\cdot)) [\alpha \omega x(1 - x)G'(y)]}{[x + (1 - x) \exp(-\alpha(\cdot))]^2} \\ 1 & 0 \end{bmatrix}$$

526 where $(\cdot) = (1 - \omega)R(x) + \omega R(y) - (1 - \omega)L(x) - \omega L(y)$. So, $\det(J) = 0 \Rightarrow \alpha \omega x(1 - x)g'(y) = 0$ and if we consider the expres-
 527 sions of payoff functions given in (4) then we have $g(x) = R(x) - L(x) = -ax^2 + (a - c)x - d$, hence $g'(x) = -2ax + a - c$. So,
 528 $LC_{-1} : \alpha \omega x(1 - x)(-2ay + a - c) = 0$, i.e. $y = \frac{1}{2}(1 - \frac{c}{a})$, and $LC = T(LC_{-1})$ is given by

$$\begin{cases} y(t+1) = x(t) \\ x(t+1) = \frac{y(t+1)}{y(t+1) + (1 - y(t+1)) \exp\{-\alpha[(1 - \omega)g(y(t+1)) + \omega g(y(t))]\}} \end{cases}$$

529 with $y(t) = \frac{1}{2}(1 - \frac{c}{a})$, hence the analytic expression of LC is given by

$$LC : x = \frac{y}{y + (1 - y) \exp\{-\alpha[(1 - \omega)g(y) + \omega g(\frac{1}{2}(1 - \frac{c}{a}))]\}}$$

530 **References**

531 Abraham, R., Gardini, L., Mira, C., 1997. *Chaos in Discrete Dynamical Systems (A Visual Introduction in 2 Dimensions)*. Springer-Verlag, New York, NY.
 532 Agliari, A., Bischi, G.I., Gardini, L., 2002. Some methods for the global analysis of dynamic games represented by noninvertible maps. In: Puu, T., Sushko, I.
 533 (Eds.), *Oligopoly Dynamics: Models and Tools*. Springer, pp. 31–83.
 534 Allport, F., 1924. *Social Psychology*. Houghton Mifflin, The Riverside Press, Cambridge, MA.
 535 Arthur, W.B., 1989. Competing technologies, increasing returns, and lock-in by historical events. *Econ. J.* 97, 642–665.
 536 Arthur, W.B., 1994. *Increasing Returns and Path Dependence in the Economy*. University of Michigan Press, Ann Arbor.
 537 Arthur, W.B., 1994. Inductive reasoning and bounded rationality. *Am. Econ. Rev.* 84, 406–411.

- 538 Arthur, W. B., 2013. Complexity Economics: A Different Framework for Economic Thought. SFI WORKING PAPER: 2013-04-012.
- 539 Benckendorff, P., Pearce, P., 2012. The psychology of events. In: Page, S., Connell, J. (Eds.), *Handbook of Events*. Routledge, New York, NY.
- 540 Bischi, G., Chiarella, C., Gardini, L., 2010. *Nonlinear Dynamics in Economics, Finance and Social Sciences: Essays in Honour of John Barkley Rosser*. Springer.
- 541 Bischi, G., Chiarella, C., Sushko, I., 2012. *Global Analysis of Dynamic Models in Economics and Finance: Essays in Honour of Laura Gardini*. Springer Science & Business Media.
- 542 Bischi, G., Lamantia, F., 2002. Nonlinear duopoly games with positive cost externalities due to spillover effects. *Chaos, Solitons Fractals* 13, 805–822.
- 543 Bischi, G., Merlone, U., 2017. Evolutionary minority games with memory. *J. Evol. Econ.* 27 (5), 859–875. doi:10.1007/s00191-017-0526-4.
- 544 Bischi, G.I., Dawid, H., Kopel, M., 2003. Gaining the competitive edge using internal and external spillovers: a dynamic analysis. *J. Econ. Behav. Organ.* 27, 2171–2193.
- 545 Bischi, G.I., Dawid, H., Kopel, M., 2003. Spillover effects and the evolution of firm clusters. *J. Econ. Behav. Organ.* 50, 47–75.
- 546 Bischi, G.I., Merlone, U., 2009. Global dynamics in binary choice models with social influence. *J. Math. Sociol.* 33 (4), 277–302.
- 547 Bischi, G.I., Merlone, U., 2010. Binary choices in small and large groups: a unified model. *Physica A: Statistical Mechanics and its Applications*, 389 (4), 843–853.
- 548 Bolle, F., 2014. On a Class of Threshold Public Goods Games: With Applications to Voting and the Kyoto Protocol. Discussion Paper, European University Viadrina, Department of Business Administration and Economics, 345.
- 549 Buchanan, J.M., 1965. An economic theory of clubs. *Economica*, New Series 32 (125), 1–14.
- 550 Cabrales, A., Sobel, J., 1992. On the limit points of discrete selection dynamics. *J. Econ. Theory* 57, 407–419.
- 551 Camerer, C., Loewenstein, G., 2004. Behavioral economics: past, present, and future. In: Camerer, G., Colin, F., Rabin, M. (Eds.), *Advances in Behavioral Economics*. Princeton University Press, Princeton, NJ, pp. 3–51.
- 552 Cavagna, A., 1999. Irrelevance of memory in the minority game. *Phys. Rev. E* 59 (4), 3783–3786.
- 553 Challet, D., Marsili, M., 2000. Relevance of memory in minority games. *Phys. Rev. E* 62 (2), 1862–1868.
- 554 Chiarella, C., 1990. The Elements of a Nonlinear Theory of Economic Dynamics. *Lecture Notes in Economics and Mathematical Systems*.
- 555 Chiarella, C., 1991. The Birth of Limit Cycles in Cournot Oligopoly Models with Time Delays. Working Paper Series, 11. Finance Discipline Group, UTS Business School, University of Technology, Sydney.
- 556 Chiarella, C., He, X.-Z., Hommes, C., 2006. Moving average rules as a source of market instability. *Physica A: Statistical Mechanics and its Applications*, 370 (1), 12–17.
- 557 Chiarella, C., Szidarovszky, F., 2003. Bounded continuously distributed delays in dynamic oligopolies. *Chaos, Solitons Fractals* 18 (5), 977–993. [https://doi.org/10.1016/S0960-0779\(03\)00067-5](https://doi.org/10.1016/S0960-0779(03)00067-5).
- 558 Chiarella, C., Szidarovszky, F., 2004. Dynamic oligopolies without full information and with continuously distributed time lags. *J. Econ. Behav. Organiz.* 54 (4), 495–511. <https://doi.org/10.1016/j.jebo.2003.01.006>.
- 559 Dieci, R., He, X., Hommes, C., 2014. *Nonlinear Economic Dynamics and Financial Modelling: Essays in Honour of Carl Chiarella*. Springer.
- 560 Dindo, P., 2005. A tractable evolutionary model for the minority game with asymmetric payoffs. *Physica A: Statistical Mechanics and its Applications*, 335 (4), 110–118.
- 561 Dixit, A., 2006. Thomas Schelling's contributions to game theory. *Scand. J. Econ.* 180 (2), 213–229.
- 562 Dohhani, A., Inaba, T., Osaka, H., 2007. Time and space in economics. In: Asada, T., Ishikawa, T. (Eds.), *Business Cycles Dynamics. Models and Tools*. Springer, New York, NY, pp. 129–143.
- 563 Elaydi, S., 1995. *An Introduction to Difference Equations*. Springer-Verlag, New York, NY.
- 564 Fazeli, A., Jadbabaie, A., 2012. Duopoly pricing game in networks with local coordination effects. *Maui, Hawaii*, pp. 74–79.
- 565 Gandolfo, G., 2010. *Economic Dynamics*. Springer-Verlag, New York, NY.
- 566 Granovetter, M., 1978. Threshold models of collective behavior. *Am. J. Sociol.* 83 (1), 1420–1443.
- 567 Granovetter, M., Soong, R., 1983. Threshold models of diffusion and collective behavior. *J. Math. Sociol.* 9 (3), 165–179.
- 568 Grebogi, C., Ott, E., Yorke, J.A., 1983. Crises, sudden changes in chaotic attractors, and transient chaos. *Physica D: Nonlinear Phenomena*, 7 (1), 181–200.
- 569 Guckenheimer, J., Holmes, P., 1983. *Nonlinear Oscillations, Dynamical Systems, and Bifurcations of Vector Fields*. Springer-Verlag, New York, NY.
- 570 Gumowski, I., Mira, C., 1980. *Dynamique Chaotique*. Cepadues Editions, Toulouse.
- 571 Hofbauer, J., Sigmund, K., 2003. Evolutionary game dynamics. *Bull. Am. Math. Soc.* 40 (4), 479–519.
- 572 Hovi, J., 1986. Binary games as models of public goods provision. *Scan. Polit. Stud.* 9 (4), 337–360.
- 573 Laffont, J., 2008. Externalities. In: Durlauf, S.N., Blume, L.E. (Eds.), *The New Palgrave Dictionary of Economics*. Palgrave Macmillan, Basingstoke, UK.
- 574 Leijonhufvud, A., 1973. Effective demand failures. *Swedish J. Econ.* 75 (1), 27–48.
- 575 Liebowitz, S.J., Margolis, S.E., 1995. Path dependence, lock-in and history. *J. Law, Econ. Organ.* 11, 205–226.
- 576 Lorenz, H., 1993. *Nonlinear Dynamical Economics and Chaotic Motion*, second ed. Springer-Verlag, New York, NY.
- 577 Mahajan, V., Muller, E., Bass, F.M., 1990. New product diffusion models in marketing: a review and directions for research. *J. Mark.* 54 (1), 1–26.
- 578 Mankiw, N.G., Taylor, M., 2014. *Economics*, third Cengage Learning EMEA, Andover, UK.
- 579 Marshall, A., 1920. *Principles of Economics: An Introductory Volume*, eight ed. Macmillan, London, UK.
- 580 Medio, A., Lines, M., 2001. *Nonlinear Dynamics*. Cambridge University Press, Cambridge, UK.
- 581 Mira, C., Gardini, L., Barugola, A., Cathala, J., 1996. *Chaotic Dynamics in Two-Dimensional Noninvertible Maps*. World Scientific.
- 582 Morgan, M., 2009. What makes a good festival? Understanding the event experience. *Event Manage.* 12 (2), 81–93.
- 583 Pierson, P., 2000. Increasing returns, path dependence and the study of politics. *Am. Polit. Sci. Rev.* 94 (2), 251–267.
- 584 Schelling, T.C., 1973. Hockey helmets, concealed weapons, and daylight saving: a study of binary choices with externalities. *J. Conflict Resolut.* 17 (3), 381–428.
- 585 Schelling, T.C., 1978. *Micromotives and Macrobehavior*. W. W. Norton, New York, NY.
- 586 Schreyögg, G., Sydow, J., Holtmann, P., 2011. How history matters in organisations: the case of path dependence. *Manage. Organ. Hist.* 6 (1), 81–100.
- 587 Thaler, R., Mullainathan, S., 2001. Behavioral economics. In: Smelser, N., Bates, P. (Eds.), *International Encyclopedia of the Social and Behavioral Sciences*. Elsevier, Oxford, UK.
- 588 Thaler, R.H., 2016. Behavioral economics: past, present, and future. *Am. Econ. Rev.* 106 (7), 1577–1600.
- 589 van Ginneken, J., 2003. *Collective Behavior Public Opinion*. Lawrence Erlbaum Associates, Mahwah, NJ.